Supplementary

Negative Linear Compressibility of Formate Crystals from the Viewpoint of Quantum Electronic Pressure

Y.V. Matveychuk, S.A. Sobalev, P.I. Borisova, E.V. Bartashevich, V.G. Tsirelson

For a small deformations of 3D solid, the generalized Hooke's law, presented in tensor form and relating the components of the stress tensors σ_{ij} and strain tensors ε_{ij}, is valid. The stiffness tensor (tensor of elastic constants), c_{ijkl}, inverse to the tensor of elastic moduli, S_{ijkk}, is more convenient for the analysis of elastic properties of solid, read as [1]:

$$\sigma_{ij} = \sum_{k=1}^{3} \sum_{l=1}^{3} c_{ijkl}\varepsilon_{kl}, \quad i, j = 1,2,3. \tag{S1}$$

Linear compressibility is obtained by applying an isotropic stress that corresponds to pressure p, in such a way that in tensor form $\varepsilon_{ij} = -pS_{ijkk}$, and considering that the stretch in a certain direction is $\varepsilon_{ij}a_i a_j$, written in vector form as

$$\beta(\theta, \varphi) = S_{ijkk}a_i a_j \tag{S2}$$

где i, j, k – indices of the tensor component corresponding to the certain direction.

To analyze the stiffness tensor and calculate the spatial dependences of elastic moduli, the online tool ELATE [2] was developed. ELATE uses a 6x6 symmetric matrix of stiffness tensor components in Voigt notation, expressed in GPa, as input. Initially, the tool calculates and displays the generalized mechanical properties: bulk modulus, Young's modulus, shear modulus and Poisson's ratio according to the averaging schemes of Voigt, Reuss and Hill. It also calculates six eigenvalues of the stiffness tensor to test the condition of structure mechanical stability. Linear compressibility can be represented as a 3D parametric surface. ELATE allows to visualize the dependence of a modulus value on a spatial direction in which it is measured, as well as their 2D representations in the (xy), (xz), (yz) planes.
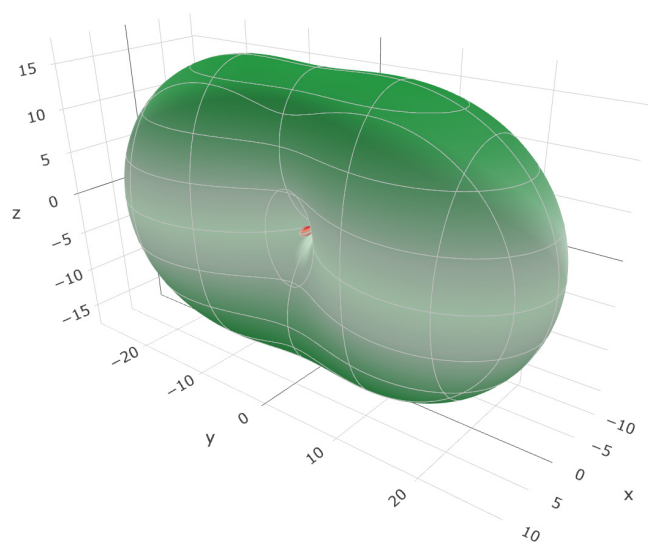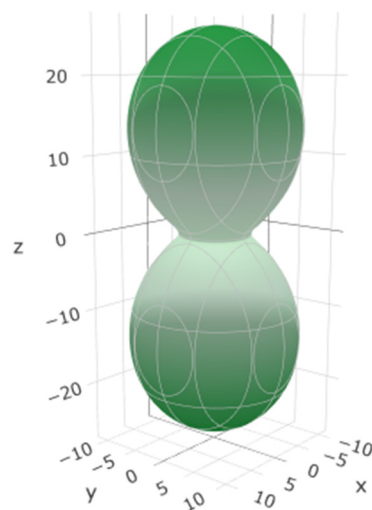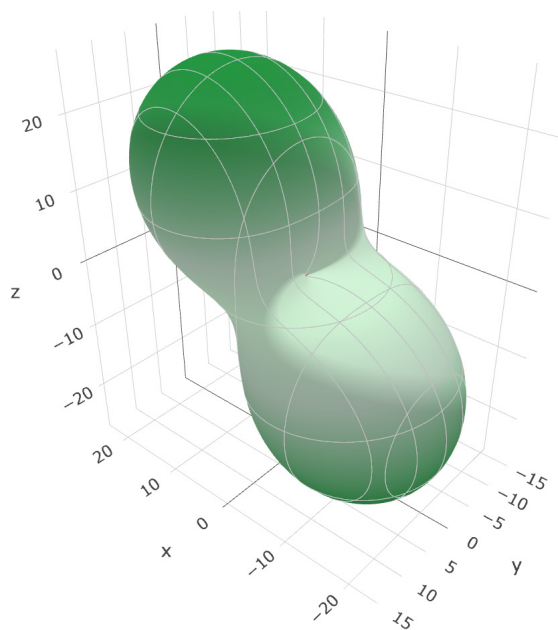
a)   b)
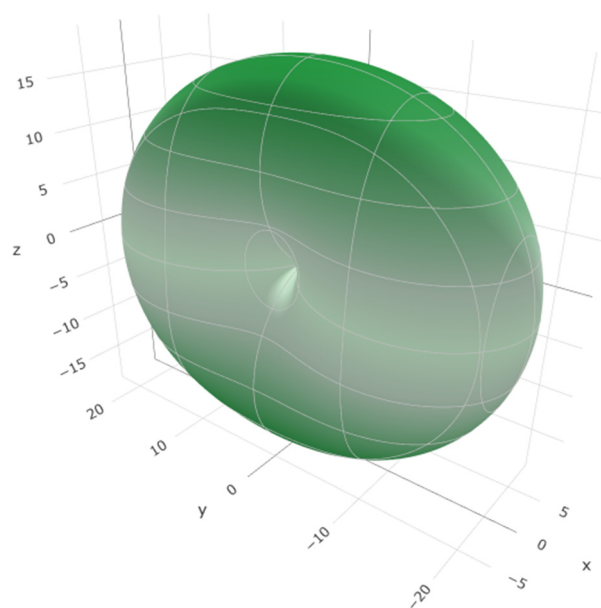
Figure S1. Spatial dependencies of linear compressibility for the calcium formate α-phase crystals (a) and calcium formate β-phase crystals (b). All axes in TPa^{-1}.

a)   b)

Figure S2. Spatial dependencies of linear compressibility for the cadmium formate crystals (a) and sodium formate crystals (b). All axes in TPa^{-1}.

Table S1. Comparison of the experimental and calculated crystal cell parameters for the equilibrium forms of considered crystals.

Crystal form	SG	a, Å	b, Å	c, Å	β	V_{cell}, Å^3	RMSD, Å
α-calcium formate (exp, CSD) [3]	Pcab	10.16	13.38	6.27	90	852.8	0.19
α-calcium formate (calc)		10.52	13.00	6.20	90	847.7	
Cadmium formate (exp) [4]	C2/c	11.61	6.19	12.41	112.5	823.5	0.26
Cadmium formate (calc)		12.03	6.09	12.56	117.2	818.2	
Cadmium formate (calc with pob-DZVP basis set)		11.97	6.04	12.38	116.0	804.6	0.24
Sodium formate (exp) [5]	C2/c	6.24	6.75	6.10	116.6	229.5	0.04
Sodium formate (calc)		6.16	6.90	6.05	117.1	228.9	
β-calcium formate (exp) [6]	P4$_1$2$_1$2	6.78	6.78	9.45	90	434.0	0.19
β-calcium formate (calc)		6.90	6.90	9.06	90	430.9	

Note. RMSD is the standard deviation of the calculated atoms coordinates in a crystal cell from the experimental data.

Table S2. Comparison of the mechanical characteristics of the equilibrium forms of considered crystals.

Crystal	Bulk modulus K, GPa	LC_{min}, TPa^{-1}	LC_{max}, TPa^{-1}	$LC_N(min)$ calc	$LC_N(min)$ exp	$LC_N(max)$ calc	$LC_N(max)$ exp
α-calcium formate (calc)	27.8	-3.29	27.33	-0.09	-0.21 [7]	0.76	0.74 [7]
Cadmium formate (calc)	28.7	-1.23	30.32	-0.04	-0.26 [7]	0.87	1.06 [7]
Cadmium formate (calc, pob-DZVP basis set)	29.5	-3.82	36.24	-0.11		1.07	
Sodium formate (calc)	27.6 (26.0 [8])	-0.04	21.73	-0.001		0.60	
β-calcium formate (calc)	33.2	4.66	26.13	0.15		0.87	

Note. $LC_N(min)$ and $LC_N(max)$ are the minimal and maximal linear compressibility, normalized with respect to the bulk compressibility LC_V: $LC_N(min) = LC_{min}/LC_V$ and $LC_N(max) = LC_{max}/LC_V$, where $LC_V = 1000/K$ TPa^{-1}, K – bulk modulus in GPa.
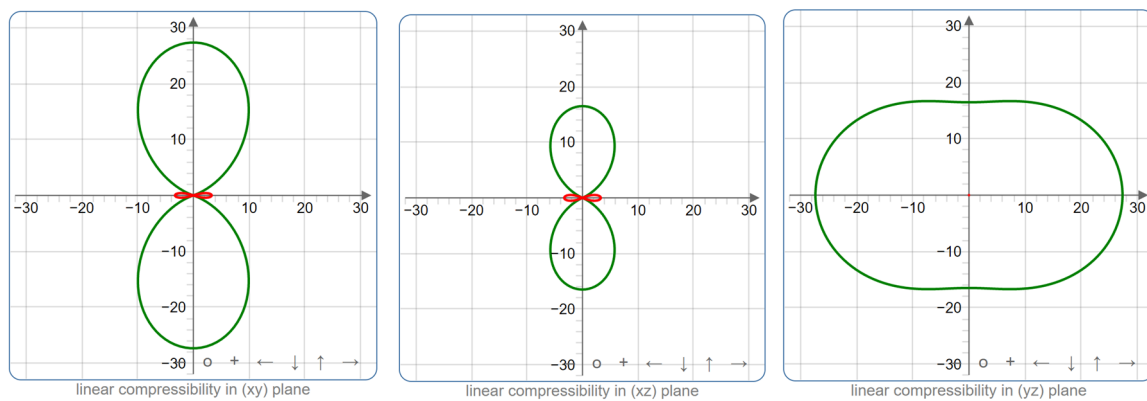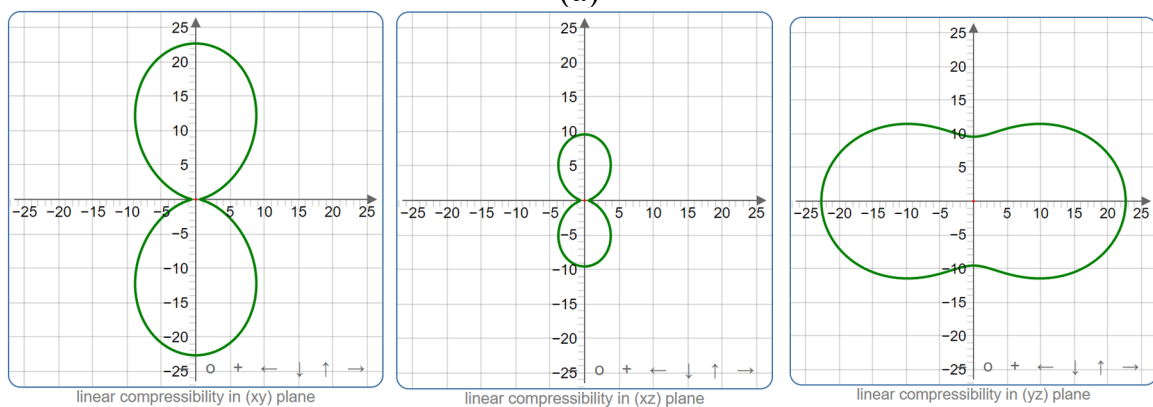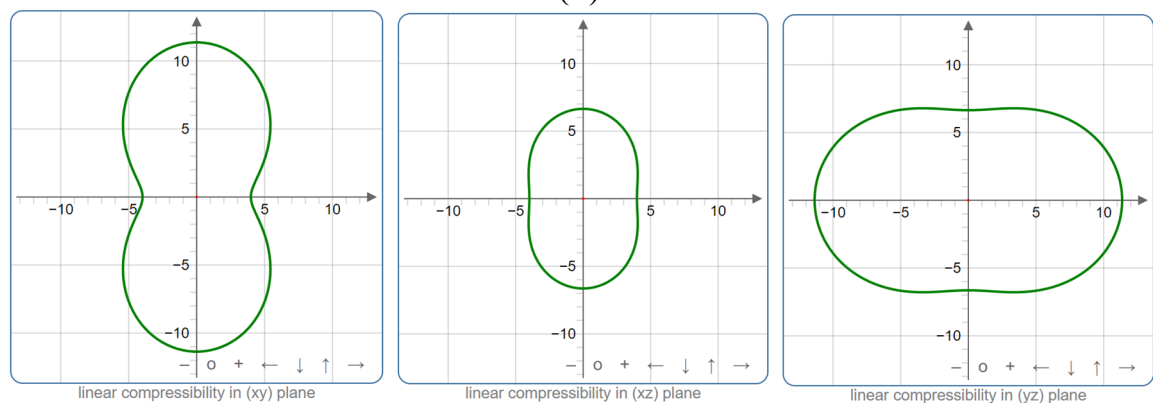
Figure S3. Change of the spatial dependences of linear compressibility for the calcium formate α-phase crystals under increasing pressure: a) 0 GPa; b) 3.25 GPa; c) 4.75 GPa. All axes in TPa^{-1}.

Table S3. Change of crystal cell parameters of the calcium formate α-phase crystals at hydrostatic compression.

Pressure, GPa	a, Å	b, Å	c, Å	V_{cell}, Å^3
0	10.5198	13.0026	6.1972	847.6759
1	10.5433	12.6931	6.1099	817.6674
2	10.5535	12.4461	6.0391	793.2335
3	10.5591	12.2234	5.9794	771.7552
3.25	10.5607	12.1619	5.9658	766.2412
3.5	10.5603	12.0782	5.9537	759.3908
4	10.5475	11.9561	5.9303	747.8522
4.75	10.5211	11.8449	5.9009	735.3813
5	10.5120	11.8125	5.8924	731.6716
6	10.4749	11.6989	5.8606	718.1908

Table S4. Linear compressibility and bulk modulus values of the calcium formate α-phase crystals at hydrostatic compression.

Pressure, GPa	Bulk modulus, GPa	LC_{min}, TPa^{-1}	LC_{max}, TPa^{-1}	A_{LC}
0	27.8	-3.30	27.33	–
1	33.4	-1.31	21.37	–
2	37.4	-0.33	18.49	–
3	37.6	0.18	19.78	108.99
3.25	34.5	0.62	22.70	36.66
3.5	31.4	2.18	23.59	10.82
4	39.2	3.68	15.33	4.17
4.75	46.7	3.99	11.37	2.85
5	48.4	4.01	10.79	2.69

Table S5. Change of crystal cell parameters of the calcium formate β-phase crystals at hydrostatic compression.

Pressure, GPa	a, Å	c, Å	V_{cell}, Å³
0	6.8978	9.0566	430.9068
0.5	6.8814	8.9477	423.7067
1	6.8669	8.8504	417.3361
1.5	6.8530	8.7648	411.6207
2	6.8399	8.6860	406.3614
3	6.8153	8.5454	396.9265
4	6.7927	8.4208	388.5450
5	6.7720	8.3040	380.8188
6	6.7576	8.1719	373.1711

Table S6. Linear compressibility and bulk modulus values of the calcium formate β-phase crystals at hydrostatic compression.

Pressure, GPa	Bulk modulus, GPa	LC_{min}, TPa^{-1}	LC_{max}, TPa^{-1}	A_{LC}
0	33.2	4.66	26.13	5.61
0.5	36.2	4.50	22.90	5.09
1	39.0	4.33	20.58	4.76
1.5	41.7	4.19	18.68	4.46
2	44.2	4.06	17.27	4.26
3	44.4	4.65	15.12	3.26
4	42.3	5.69	13.18	2.32
5	40.4	6.45	12.38	1.92
6	40.7	6.10	12.80	2.10

Table S7. Change of crystal cell parameters of the cadmium formate crystals at hydrostatic compression.

Pressure, GPa	a, Å	b, Å	c, Å	β	V_{cell}, Å³
0	12.0265	6.0878	12.5605	117.1681	818.1553
0.1	12.0119	6.0807	12.5559	117.3124	814.8591
0.25	11.9932	6.0708	12.5472	117.5097	810.2574
0.35	11.9811	6.0640	12.5417	117.6362	807.2531
0.5	11.9630	6.0542	12.5336	117.8199	802.8452
1	11.9054	6.0244	12.5076	118.3706	789.3341
1.5	11.8512	5.9997	12.4805	118.8532	777.2328
2	11.7986	5.9773	12.4544	119.2724	766.1765
2.5	11.7494	5.9577	12.4282	119.6455	756.0930
3	11.7033	5.9409	12.4006	119.9838	746.7992

Table S8. Linear compressibility and bulk modulus values of the cadmium formate crystals at hydrostatic compression.

Pressure, GPa	Bulk modulus, GPa	LC_{min}, TPa⁻¹	LC_{max}, TPa⁻¹	A_{LC}
0	28.7	-1.23	30.32	–
0.1	29.2	-0.80	29.08	–
0.25	30.0	-0.26	27.41	–
0.35	30.5	0.04	26.57	730.72
0.5	31.3	0.42	25.30	60.63
1	33.6	1.27	22.48	17.66
1.5	35.9	1.80	20.52	11.38
2	38.1	2.19	18.93	8.63
2.5	40.3	2.49	17.54	7.05
3	42.5	2.73	16.31	5.98

Table S9. Change of crystal cell parameters of the sodium formate crystals at hydrostatic compression.

Pressure, GPa	a, Å		b, Å		c, Å		β		V_{cell}, Å^3	
	calc	exp	calc	exp	calc	exp	calc	exp	calc	exp
0	6.1642	6.24	6.8997	6.75	6.0474	6.10	117.1374	116.61	228.8847	229.5
0.1	6.1640	6.25	6.8852	6.75	6.0395	6.17	117.1936	116.09	227.9867	234
0.5	6.1677	6.25	6.8240	6.68	6.0088	6.14	117.4295	–	224.4686	230
1	6.1797	6.25	6.7414	6.61	5.9730	6.10	117.7461	117.00	220.2269	225
1.5	6.1896	6.25	6.6682	6.57	5.9388	6.07	118.0477	–	216.3281	223
2	6.1940	6.24	6.6076	6.53	5.9063	6.05	118.2893	–	212.8576	219
3	6.1973	6.23	6.5046	6.46	5.8461	6.00	118.6820	–	206.7451	214
3.5	6.1992	6.21	6.4570	6.42	5.8178	5.98	118.8579	117.86	203.9586	211
4	6.2031	6.20	6.4093	6.40	5.7889	5.96	119.0382	–	201.2190	208
4.5	6.2228	6.19	6.3435	6.38	5.7500	5.94	119.3536	–	197.8364	207
5	6.2260	6.17	6.3022	6.37	5.7253	5.91	119.5532	–	195.4198	204
5.5	6.2255	6.15	6.2671	6.36	5.7043	5.89	119.7244	–	193.2730	202
6	6.2235	–	6.2354	–	5.6851	–	119.8789	–	191.2929	–
7	6.2178	–	6.1791	–	5.6501	–	120.1524	–	187.7065	–

Note. Experimental data on crystals under pressure are taken from [10].

Table S10. Linear compressibility and bulk modulus values of the sodium formate crystals at hydrostatic compression.

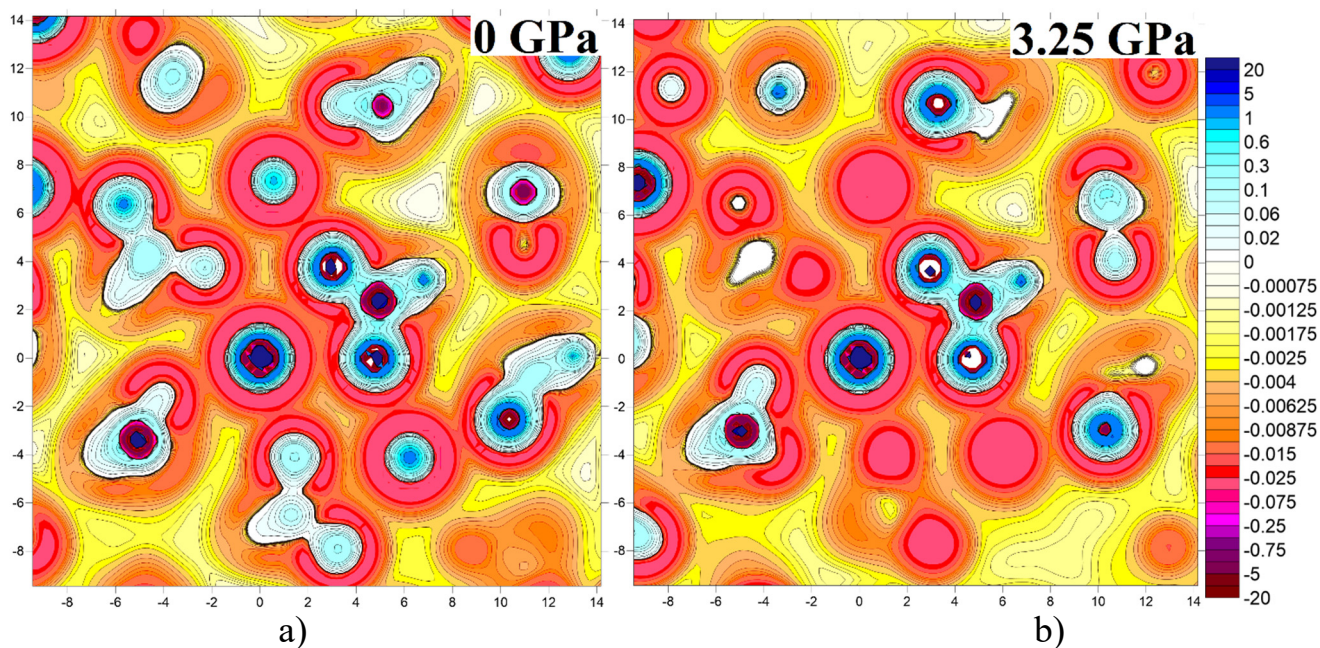| Pressure, GPa	Bulk modulus, GPa	LC_{min}, TPa^{-1}	LC_{max}, TPa^{-1}	A_{LC}
0	27.6	-0.05	21.73	–
0.1	27.9	-0.46	21.98	–
0.5	29.1	-2.37	23.58	–
1	30.7	-3.16	23.25	–
1.5	33.1	-1.08	19.23	–
2	35.3	-0.02	16.76	–
3	38.9	0.10	14.87	151.26
3.5	40.2	-0.23	14.64	–
4	39.0	-2.13	16.60	–
4.5	39.8	-2.51	16.56	–
5	45.5	0.22	12.33	56.19
5.5	48.4	0.77	11.12	14.43
6	50.9	1.07	10.26	9.60
7	55.5	1.34	9.20	6.87

Figure S4. Contour maps of $p(\mathbf{r})$ distribution in Ca…O…O plane a) in equilibrium structure and b) under the hydrostatic pressure in 3.25 GPa in **α-Ca²⁺fmt**.
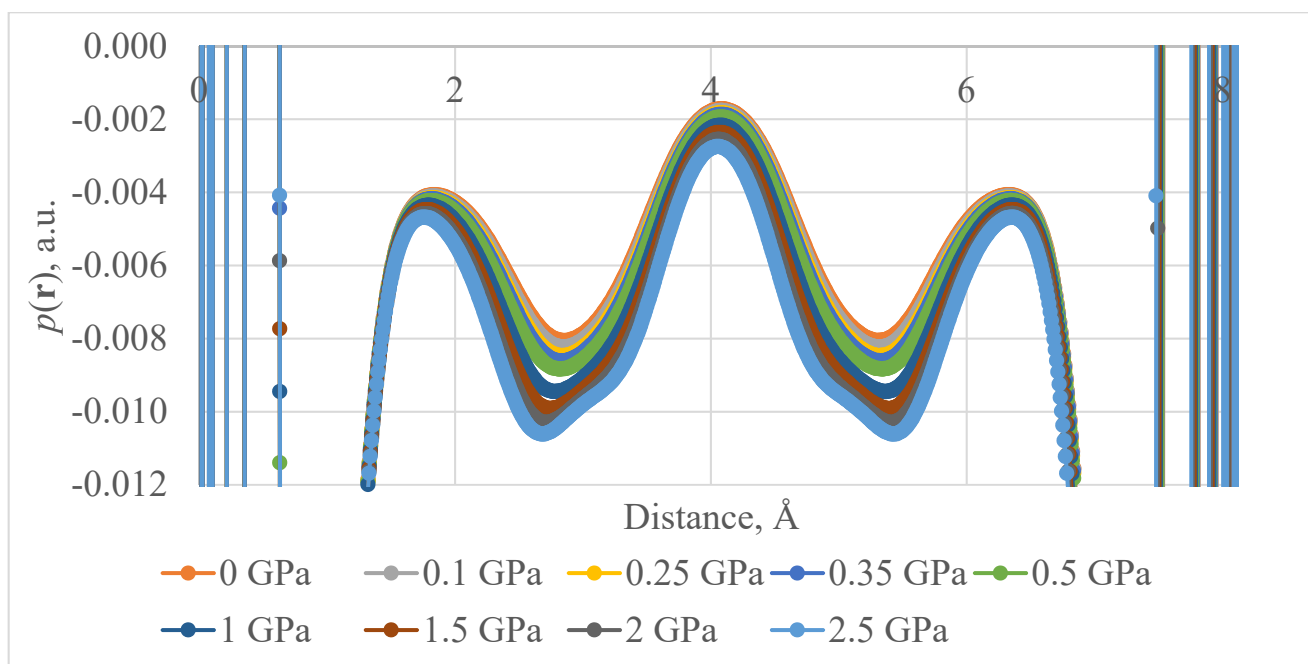

Figure S5. Change of $p(\mathbf{r})$ along the LC_{min} axis between Cd^{2+} ions in **Cd²⁺fmt** with increasing hydrostatic compression.
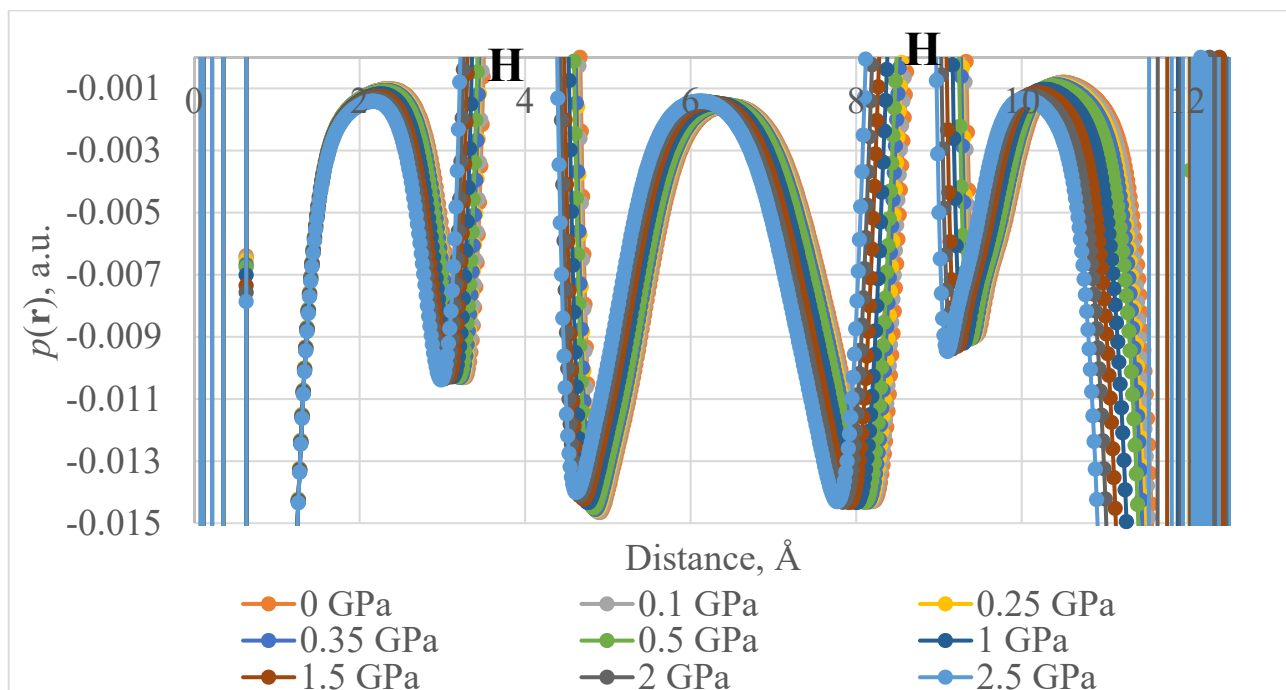
Figure S6. Change of $p(\mathbf{r})$ along LC_{max} axis between Cd^{2+} ions in **Cd^{2+}fmt** with increasing hydrostatic compression.
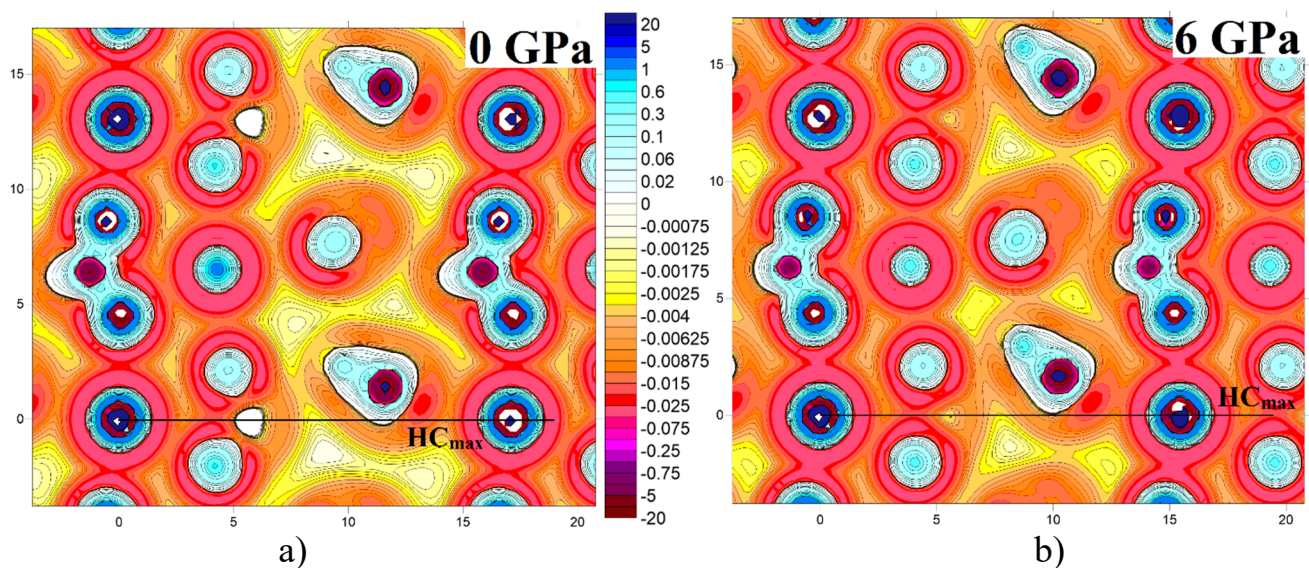

Figure S7. Contour maps of $p(\mathbf{r})$ distribution in Ca…Ca…Ca plane, coplanar LC_{max}, a) in equilibrium structure and b) under hydrostatic pressure in 6 GPa in **β-Ca^{2+}fmt**.
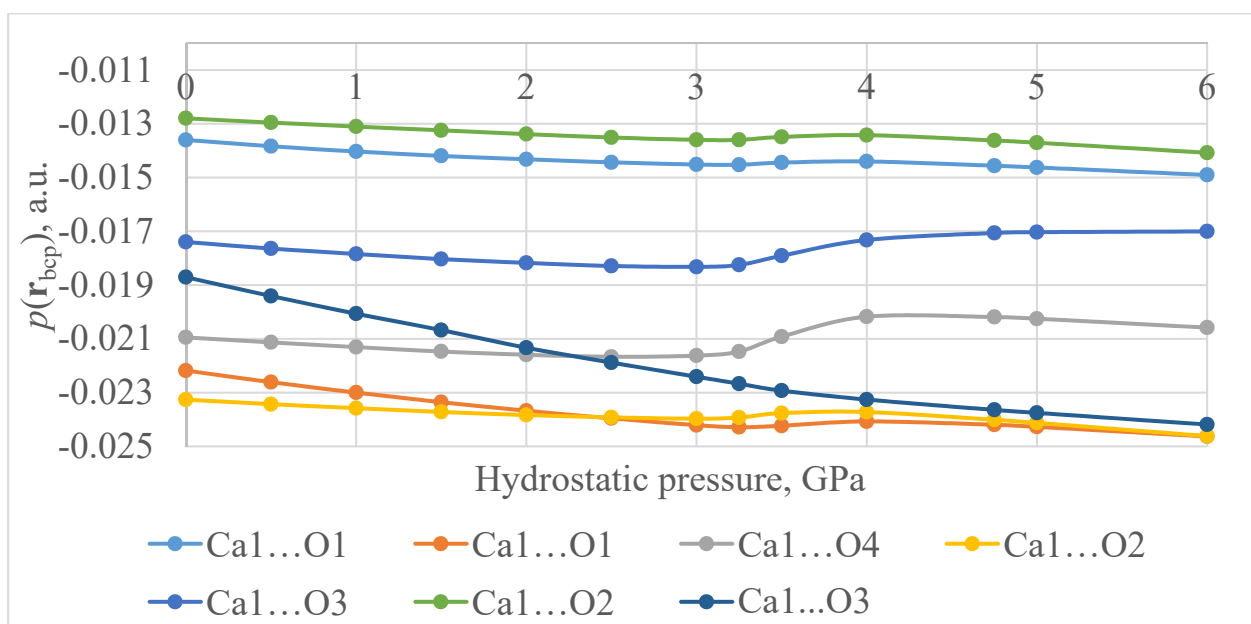
Figure S8. Change of $p(r_{bcp})$ of Ca…O ionic bonds in **α-Ca²⁺fmt** with increasing hydrostatic pressure.
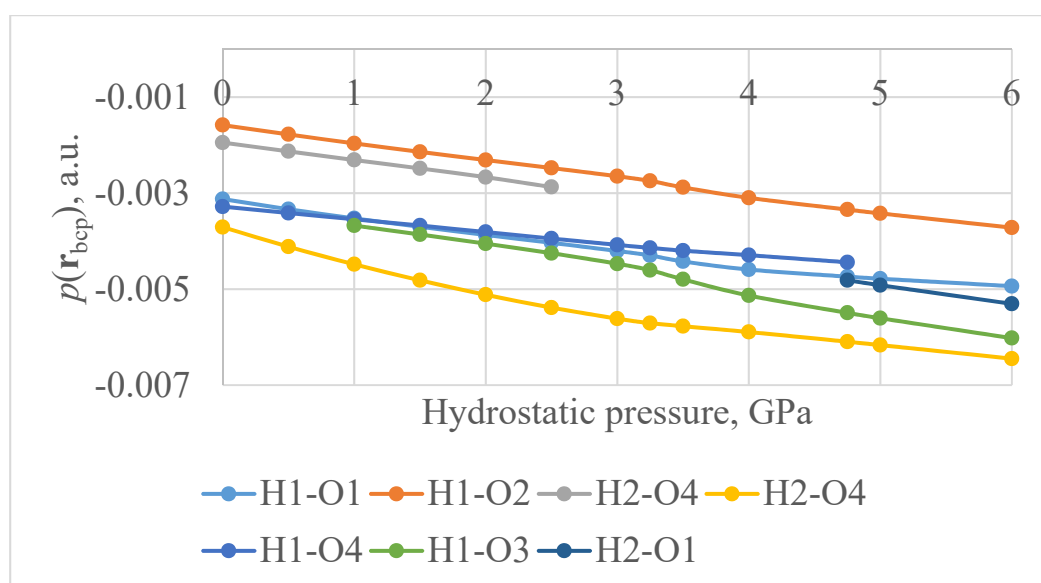

Figure S9. Change of $p(r_{bcp})$ of H…O hydrogen bonds in **α-Ca²⁺fmt** with increasing hydrostatic pressure.

Figure S10. Change of $p(r_{bcp})$ of H…O hydrogen bonds in **β-Ca^{2+}fmt** with increasing hydrostatic pressure.

Figure S11. Change of $p(r_{bcp})$ of H…O hydrogen bonds in **Cd^{2+}fmt** with increasing hydrostatic pressure.

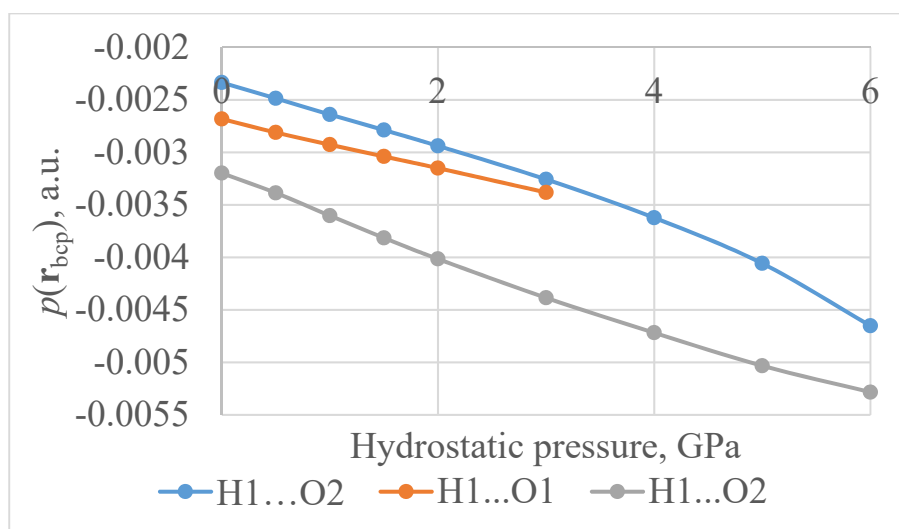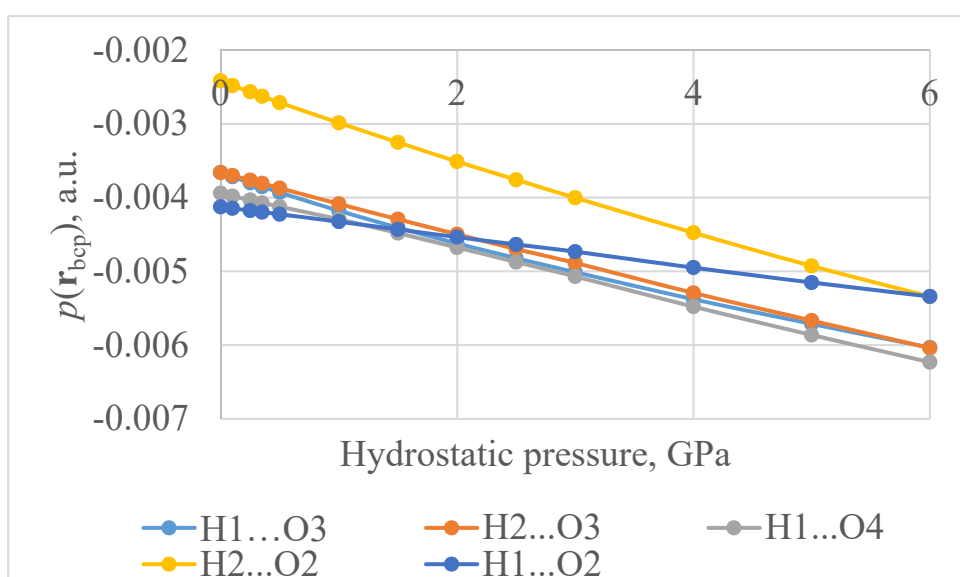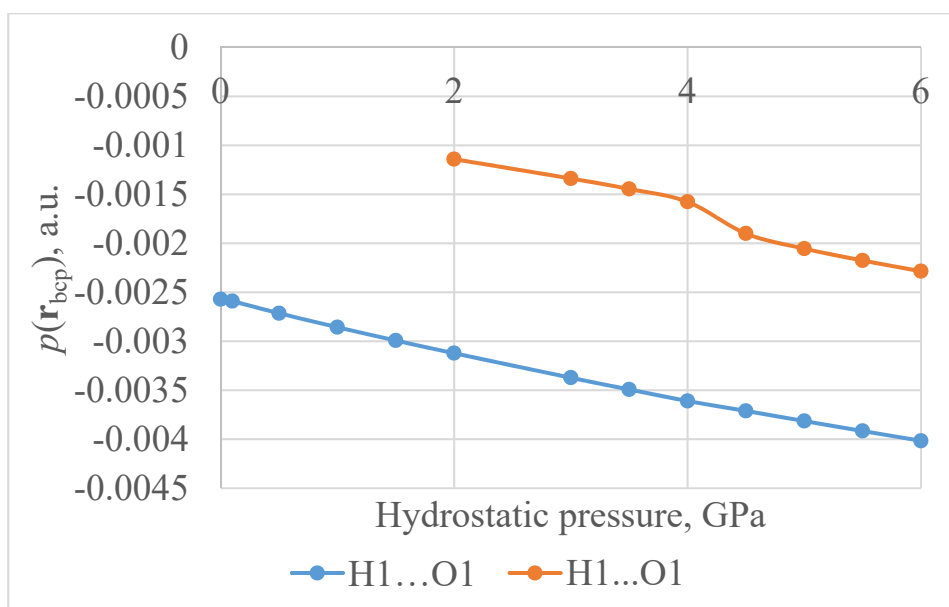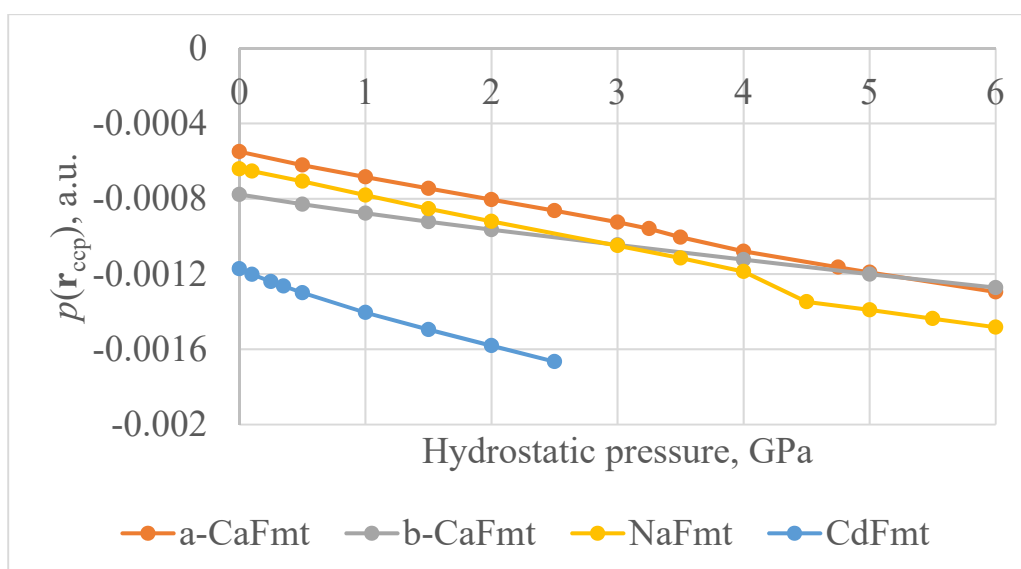Figure S12. Change of $p(r_{bcp})$ of H…O hydrogen bonds in **Na⁺fmt** with increasing hydrostatic pressure.

Figure S13. Change of $p(\mathbf{r}_{ccp})$ in formate crystals with increasing hydrostatic pressure.

Table S11. Values of absolute change of $p(\mathbf{r})$, Δp, and relative change, $\Delta p\%$ of ionic bonds with increasing hydrostatic compression up to 6 GPa.

α-Ca^{2+}fmt		
Bond	Δp	$\Delta p\%$
Ca$_1$...O$_1$	0.0013	9.8
Ca$_1$...O$_1$	0.0024	11.04
Ca$_1$...O$_4$	0.00036	1.74
Ca$_1$...O$_2$	0.0014	5.82
Ca$_1$...O$_3$	0.0004	2.26
Ca$_1$...O$_2$	0.0013	10.01
Ca$_1$...O$_3$	**0.0055**	**29.30**
β- Ca^{2+}fmt		
Bond	Δp	$\Delta p\%$
Ca$_1$...O$_2$	0.0029	**40.02**
Ca$_1$...O$_1$	0.0021	14.66
Ca$_1$...O$_1$	**0.0043**	20.11
Ca$_1$...O$_2$	0.0042	17.76
Na$^+$fmt		
Bond	Δp	$\Delta p\%$
Na$_1$...O$_1$	0.0032	37.53
Na$_1$...O$_1$	**0.0047**	**49.40**
Na$_1$...O$_1$	0.0042	37.39
Cd^{2+}fmt		
Bond	Δp	$\Delta p\%$
Cd$_1$...O$_3$	-0.0024	**27.60**
Cd$_1$...O$_4$	-0.0011	1.98
Cd$_1$...O$_1$	-0.0025	12.14
Cd$_1$...O$_4$	**-0.0046**	21.42
Cd$_1$...O$_1$	-0.0009	4.05
Cd$_1$...O$_2$	-0.0017	6.84
Cd$_1$...O$_3$	-0.0039	15.29

Table S12. Values of absolute change of $p(\mathbf{r})$, Δp, and relative change, $\Delta p\%$ of hydrogen bonds with increasing hydrostatic compression up to 6 GPa.

Bond	Δp	$\Delta p\%$
α-Ca^{2+}fmt		
Bond	Δp	$\Delta p\%$
H_1-O_1	-0.0018	58.05
H_1-O_2	-0.0021	**135.13**
H_2-O_4	**-0.0027**	73.93
β-Ca^{2+}fmt		
Bond	Δp	$\Delta p\%$
H_1-O_2	**-0.0023**	**99.20**
H_1-O_2	-0.0021	65.20
Na$^+$fmt		
Bond	Δp	$\Delta p\%$
H_1-O_1	**0.0014**	**56.19**
Cd^{2+}fmt		
Bond	Δp	$\Delta p\%$
H_1-O_3	-0.0024	64.85
H_2-O_3	-0.0024	65.00
H_1-O_4	-0.0023	58.19
H_2-O_2	**-0.0029**	**121.18**
H_1-O_2	-0.0012	29.43

Table S13. Bond lengths, Å, for M…O and H…O bonds estimated by various calculation methods.

Bond	PBE0/pob-DZVP_rev2	HSE06/pob-DZVP_rev2	Experimental (CAFORM)
α-Ca^{2+}Fmt			
Ca$_1$…O$_1$	2.529	2.530	2.481
Ca$_1$…O$_1$	2.370	2.370	2.366
Ca$_1$…O$_4$	2.374	2.374	2.319
Ca$_1$…O$_2$	2.352	2.351	2.287
Ca$_1$…O$_3$	2.436	2.436	2.458
Ca$_1$…O$_2$	2.554	2.555	2.599
Ca$_1$…O$_3$	2.418	2.419	2.410
H$_1$…O$_1$	2.647	2.649	2.515
H$_1$…O$_2$	3.187	3.190	3.193
H$_2$…O$_4$	2.416	2.415	2.584

Bond	PBE0/pob-DZVP_rev2	-	Experimental (CAFORM05)
β-Ca^{2+}Fmt			
Ca$_1$…O$_2$	2.822	-	2.944
Ca$_1$…O$_1$	2.511	-	2.484
Ca$_1$…O$_1$	2.375	-	2.364
Ca$_1$…O$_2$	2.347	-	2.312
H$_1$…O$_2$	2.795	-	2.960
H$_1$…O$_2$	2.725	-	2.961

Bond	PBE0/pob-DZVP_rev2	-	Experimental (NAFORM06)
Na$^+$Fmt			
Na$_1$…O$_1$	2.473	-	2.492
Na$_1$…O$_1$	2.417	-	2.419
Na$_1$…O$_1$	2.381	-	2.386
H$_1$…O$_1$	2.683	-	2.695

Bond	PBE0/pob-DZVP_rev2 (dou_1998 for Cd)	PBE0/pob_DZVP_rev2 (pob-DZVP ECP for Cd)	Experimental (ZZZSGO01)
Cd^{2+}Fmt			
Cd$_1$…O$_3$	2.709	2.844	2.599
Cd$_1$…O$_4$	2.403	2.332	2.586
Cd$_1$…O$_1$	2.370	2.336	2.323
Cd$_1$…O$_4$	2.367	2.346	2.285
Cd$_1$…O$_1$	2.339	2.305	2.304
Cd$_1$…O$_2$	2.292	2.252	2.259
Cd$_1$…O$_3$	2.314	2.282	2.275
H$_1$…O$_3$	2.625	2.575	2.686
H$_2$…O$_3$	2.768	2.753	3.064
H$_1$…O$_4$	2.511	2.510	2.598
H$_2$…O$_2$	2.682	2.653	2.865
H$_1$…O$_2$	2.650	2.621	2.688

1 Nye, J. F. Physical Properties of Crystals; Clarendon Press: Oxford, 1985.

2 Gaillac, R.; Coudert, F.-X. ELATE: Elastic tensor analysis.— http://progs.coudert.name/elate. (accessed on 30 June 2023)

3 Groom, C. R.; Bruno, I. J.; Lightfoot, M. P.; Ward, S. C., The Cambridge Structural Database. Acta Crystallographica Section B 2016, 72, (2), 171-179.

4 Weber, G. The structure of anhydrous cadmium formate // Acta Cryst. B, 1980, B36, 1947-1949.

5 H. Fuess, J. Willem Bats Comparison of Observed and Calculated Densities. XII. Deformation Density in Complex Anions. II. Experimental and Theoretical Densities in Sodium Formate // Acta Cryst. B, 1982, B38, 736-743.

6 M. Matsui, T. Watanabé, N. Kamijo, R. L. Lapp and R. A. JacobsonThe structures of calcium formate [beta]-Ca(HCOO)2 and [delta]-Ca(HCOO)2, and the tetragonal mixed crystals Ca(HCOO)2-Sr(HCOO)2 // Acta Cryst. B, 1980, B36, 1081-1086.

7 R.H. Baughman, S. Stafström, C. Cui, S.O. Dantas Materials with Negative Compressibilities in One or More Dimensions // Science, 1998, 279, 5356, 1522-1524.

8 Lei Kang, Shourui Li, Bo Wang, Xiaoshuang Li The effect of high pressure on the structure and stability of sodium formate: Probed by in situ synchrotron X-ray diffraction technique // Solid State Communications, 2019, 289, 67-70.